

Dynamically Generated Synthetic Electric Fields for Photons

Petr Zapletal,^{1,2} Stefan Walter,^{2,3} and Florian Marquardt^{2,3}

¹*Cavendish Laboratory, University of Cambridge, Cambridge CB3 0HE, United Kingdom*

²*Max Planck Institute for the Science of Light, Staudtstraße 2, 91058 Erlangen, Germany*

³*Institute for Theoretical Physics, University Erlangen-Nürnberg, Staudtstraße 7, 91058 Erlangen, Germany*

Static synthetic magnetic fields give rise to phenomena including the Lorentz force and the quantum Hall effect even for neutral particles, and they have by now been implemented in a variety of physical systems. Moving towards fully dynamical synthetic gauge fields allows, in addition, for backaction of the particles' motion onto the field. If this results in a time-dependent vector potential, conventional electromagnetism predicts the generation of an electric field. Here, we show how synthetic electric fields for photons arise self-consistently due to the nonlinear dynamics in a driven system. Our analysis is based on optomechanical arrays, where dynamical gauge fields arise naturally from phonon-assisted photon tunneling. We study open, one-dimensional arrays, where synthetic magnetic fields are absent. However, we show that synthetic electric fields can be generated dynamically. The generation of these fields depends on the direction of photon propagation, leading to a novel mechanism for a photon diode, inducing nonlinear unidirectional transport via dynamical synthetic gauge fields.

The field of cavity optomechanics, addressing the interaction between light and sound, has made rapid strides in recent years [1]. Experiments have shown ground state cooling [2, 3], measurements of motion with record sensitivity [4], efficient conversion between microwave and optical photons [5], dynamics of vibrations near exceptional points [6], and the control of single phonons [7], to name but a few achievements.

Due to the optomechanical interaction, mechanical vibrations can change light frequency. During this process, the mechanical oscillation phase is imparted onto light field. In this way, optomechanics can be used as a natural means to generate synthetic magnetic fields for photons, as was first suggested in Refs. [8, 9]. Together with reservoir engineering [10], these ideas form the theoretical basis underlying a recent series of pioneering experiments on optomechanical nonreciprocity [11–16]. While those still operate in few-mode setups, future extensions to optomechanical arrays (of the type proposed in [17–20]) will enable studies of photon transport on a lattice in presence of an arbitrary tunable synthetic magnetic field [9]. A similar optomechanical design underlies the first proposal for engineered topological phonon transport in any platform [21]. All of these developments tie into the much wider field of synthetic magnetic fields and topologically protected nonreciprocal transport, first envisaged and implemented for cold atoms [22–25] and then for photons [26–32], phonons [21, 33–38], and other platforms [39, 40].

In these works, gauge fields are fixed by external parameters, e.g., the phases of external driving beams. It was understood only recently that optomechanics provides a very natural platform for creating *dynamical* classical gauge fields [41]: if the mechanical resonator is not driven externally but rather undergoes limit-cycle oscillations, the phase of those oscillations becomes a dynamical gauge field. This field is a new degree of freedom that can be influenced by photons instead of being fixed externally. The possibility to engineer artificial dynamical

gauge fields has attracted attention also in different platforms, such as ultra-cold atoms in optical lattices [42, 43], superconducting circuits [44, 45], cavity quantum electrodynamics [46], and trapped ions [47, 48].

If the dynamics results in a time-dependent vector potential, conventional electromagnetism dictates that this describes an *electric* field. In the present work, we predict that synthetic electric fields can arise in rather elementary optomechanical systems, in a dynamical way. The scenarios in which these electric fields arise, and their physical consequences, are qualitatively different from the more conventional self-consistently generated magnetic fields discussed in our previous work [41]. They can arise even in a linear arrangement of coupled photon modes, where static vector potentials do not have any effect, since they can be gauged away. This makes them a very relevant phenomenon for present-day experimental implementations, in setups as simple as two coupled optical modes. Moreover, the appearance of electric fields turns out to depend on the direction of photon propagation. In this way, we uncover a novel mechanism for nonlinear unidirectional transport of photons (a photon diode). This works especially well in arrays, where transport is significantly suppressed in the blockaded direction.

Synthetic electric fields for photons have been analyzed previously only in the context of prescribed external driving [49, 50], i.e. not generated by dynamical gauge fields, unlike the situation studied here. In these cases, the nonlinear dynamics and non-reciprocal effects explored in our work are absent.

Dynamical gauge fields for photons. — The optomechanical interaction can be used to realize phonon-assisted photon tunneling, which, as we have shown previously, offers a natural route towards classical dynamical gauge fields for photons [41]. Photons hopping between optical modes \hat{a}_1 and \hat{a}_2 absorb or emit a phonon from a mechanical mode \hat{b} . A pictorial representation of this process is shown in Fig. 1a. Many implementa-

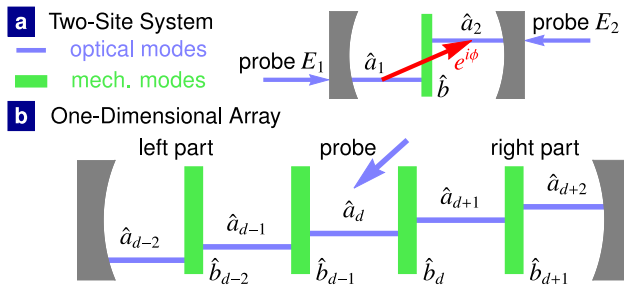


FIG. 1. An optomechanical setup exhibiting dynamically generated synthetic electric fields for photons. (a) A cavity with a movable membrane (green rectangle) in the middle. The mechanical mode \hat{b} undergoes self-oscillations. Photons tunneling from optical mode \hat{a}_1 to \hat{a}_2 (red arrow) absorb a phonon from the mechanical oscillation, thereby acquiring a phase shift set by the oscillation phase ϕ . Photon transport through the setup can be probed by driving mode \hat{a}_1 or \hat{a}_2 . Optical frequencies are represented by the blue lines. (b) A one-dimensional array, with optical modes \hat{a}_j of increasing frequency. Mechanical modes \hat{b}_j assist tunneling between modes \hat{a}_j and \hat{a}_{j+1} . Some mode, \hat{a}_d , is driven by a laser (blue arrow), probing photon transport both towards the left and right.

tions are conceivable (including photonic crystal devices, coupled toroids, and microwave circuits [1]), but a suitable realization might simply consist of the well-known membrane-in-the-middle setup [51, 52]. The Hamiltonian is

$$\hat{H} = \sum_{j=1}^2 \nu_j \hat{a}_j^\dagger \hat{a}_j + \Omega \hat{b}^\dagger \hat{b} + J \left(\hat{b} \hat{a}_2^\dagger \hat{a}_1 + \text{h.c.} \right), \quad (1)$$

where ν_j are the optical frequencies of modes \hat{a}_j , Ω is the frequency of the mechanical oscillator and J is the tunneling amplitude [41]. In the following, we set $\hbar = 1$. The optical frequencies are detuned from one another to suppress direct tunneling between the optical modes. To select the phonon-assisted photon tunneling, the mechanical frequency is tuned to match the optical frequency difference $\Omega \approx |\nu_2 - \nu_1|$. The Hamiltonian (1) is valid within the rotating-wave approximation for $\nu_2 > \nu_1$ and $\Omega \gg \kappa, J, JB$, where κ is the photon decay rate and B is the amplitude of the mechanical oscillations: $\langle \hat{b} \rangle = B e^{i\phi} e^{-i\Omega t}$.

During the photon tunneling process $\hat{b} \hat{a}_2^\dagger \hat{a}_1$, the mechanical phase ϕ is imprinted on the photons, similar to an Aharonov-Bohm (Peierls) phase. This can be used for optomechanical generation of *static* gauge fields, as was first discussed in Ref. [9], and the scheme can be readily implemented in optomechanical crystals [53, 54] or the membrane-cavity setup [51, 52, 55]. It was realized experimentally in Ref. [14].

To implement *dynamical* gauge fields for photons, i.e., fields that are themselves dynamical degrees of freedom, the oscillation phase ϕ (the ‘‘gauge field’’) has to evolve freely, which is the case if the mechanical mode performs limit-cycle oscillations [41]. The limit-cycle oscillations

can be generated by pumping an ancillary optical mode, situated at a different frequency, on the blue sideband [56]. In a limit cycle, the mechanical oscillation phase is able to evolve according to its own dynamics. Thus the phase ϕ turns into a dynamical gauge field, being influenced by photon transport and acting back on photons. The system of Eq.(1) can be used as a building block for optomechanical arrays with dynamical gauge fields for photons, as we first proposed in Ref. [41]. We will use the equations of Ref. [41] as our starting point, to predict the new phenomenon of synthetic electric fields generated by nonlinear dynamics, giving rise to unidirectional photon transport.

The basic physics behind our results. – We start with a preview of our results, emphasizing the physical intuition. Any oscillator driven by a resonant force $F_0 \cos(\Omega t - \theta)$ will experience a drift, $\dot{\phi} \propto F_0 \cos(\phi - \theta)$, of its phase ϕ . In our case, the force is the radiation pressure oscillating at the beat note between the two optical modes, and we obtain $\dot{\phi} = -(J/B) |a_1| |a_2| \cos(\phi - \theta)$, where θ is the phase difference between the optical modes. If the forcing phase θ is kept constant, this results in a stable fixed point $\phi = \theta - \pi/2$. For a limit-cycle oscillator, that behavior is known as phase locking (injection locking) to an external drive.

However, in our case an interesting self-consistency problem arises: the phase difference $\theta = \theta_2 - \theta_1$ of the two optical modes depends on ϕ itself, as the phase ϕ is imprinted onto the photons during the phonon-assisted photon tunneling. The phase of the force thus follows the oscillation phase. We now discuss qualitatively the resulting physics, which will be bolstered by detailed analysis later. Two cases need to be distinguished, depending on which optical mode is driven by the laser (see Fig. 2a and Fig. 2b). If the *higher* optical mode (labeled ‘2’) is driven, then we find $\theta = \phi + \pi/2$. Here the crucial term $\pi/2$ comes about due to the *resonant* excitation of the lower mode via the phonon-assisted transition $2 \rightarrow 1$. Comparing with the stable fixed point for ϕ deduced above, we conclude that *any* value of ϕ is now stable.

The situation changes drastically if the *lower* optical mode is driven by the laser. Then, we find $\theta = \phi - \pi/2$, where the sign has flipped because now the roles of both modes have been interchanged (now the higher mode is excited by the phonon sideband of the driven lower mode). This corresponds to an unstable fixed point. Once ϕ tries to move away, θ will follow, such that ϕ is forever repelled. This results in a finite phase drift $\dot{\phi} \neq 0$, corresponding to an effective shift of the mechanical frequency. Thus, the phonon-assisted tunneling process towards the higher optical mode is no longer in resonance but detuned by $\dot{\phi}$. This off-resonant excitation shifts the optical phase difference according to $\theta \approx \phi - \pi/2 - \dot{\phi}/(\kappa/2)$. The equation $\dot{\phi} \propto \cos(\phi - \theta)$ can then be fulfilled at a certain value of ϕ , which has to be obtained self-consistently. This is the qualitative origin of the nonlinear dynamics that gives rise to what we will identify below as a synthetic electric field $\mathcal{E} = \dot{\phi}$ acting

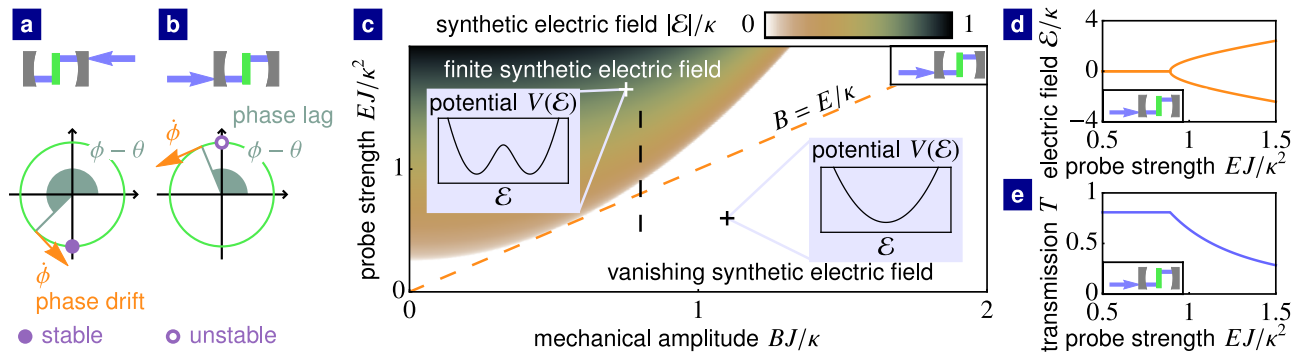


FIG. 2. Dynamically generated synthetic electric fields in the two-site system. (a,b) Phase evolution on the mechanical limit cycle (green orbit). (a) When the higher optical mode is laser-driven, the system settles into a stable fixed point, with a phase lag $\phi - \theta = -\pi/2$. (b) When the lower optical mode is driven, the phase is continuously repelled from an unstable fixed point $\phi - \theta = +\pi/2$, generating a finite synthetic electric field $\mathcal{E} = \dot{\phi} \neq 0$ acting on the photons. (c) The phase diagram. In the white region, \mathcal{E} vanishes in the steady state. If the lower-frequency mode, a_1 , is driven, \mathcal{E} bifurcates in the colored region to finite steady-state values. Their absolute values are indicated by the color scale. The blue insets show the effective potential $V(\mathcal{E})$ determining the steady-state value of \mathcal{E} . The dashed black line denotes the cut along which \mathcal{E} and the optical transmission T are plotted in (d) and (e), respectively. For the higher-frequency mode, a_2 , being driven, \mathcal{E} always vanishes for any values of the system parameters. Consequently, the transmission is never suppressed.

on the photons.

Dynamics and synthetic electric fields. — Let us analyze the dynamics of the two-site system (1) with the mechanical oscillator performing limit-cycle oscillations. The optical mode \hat{a}_j is driven by a laser of amplitude E_j at frequency $\nu_{D,j}$, probing photon transport through the system. The optical and mechanical amplitudes are assumed large enough such that quantum noise effects can be neglected, which is an excellent approximation for all existing optomechanical experiments studying nonlinear dynamics.

Following Ref. [41], the coupled classical equations of motion for the optical amplitudes $a_j = \langle \hat{a}_j \rangle$ and the mechanical phase ϕ read

$$\dot{\phi} = \Delta_M - \frac{J}{B} \text{Re} [a_1^* a_2 e^{-i\phi}], \quad (2)$$

$$\dot{a}_1 = i\Delta_1 a_1 - iE_1 - iJBe^{-i\phi} a_2 - \frac{\kappa}{2} a_1, \quad (3)$$

$$\dot{a}_2 = i\Delta_2 a_2 - iE_2 - iJBe^{i\phi} a_1 - \frac{\kappa}{2} a_2, \quad (4)$$

where $\Delta_j = \nu_{D,j} - \nu_j$ and $\Delta_M = \nu_{D,2} - \nu_{D,1} - \Omega$ are optical and mechanical detunings, respectively (switching to suitable rotating frames). The mechanical amplitude B is considered fixed, determined by the optical pump. These equations form the starting point of our analysis.

The resulting beat note gives rise to the oscillating force $F \propto J|a_1||a_2| \cos((\nu_{D,2} - \nu_{D,1})t - \theta)$ acting on the mechanical oscillator, as can be deduced from the Hamiltonian (1). While the effect of this on the large mechanical amplitude B is negligible, the mechanical phase feels the drift term $\dot{\phi} = -\frac{J}{B}|a_1||a_2| \cos(\phi - \theta)$, according to Eq. (2) (see Ref. [57] for more details).

In contrast, if only one mode is driven, no external phase is imprinted. The mechanical oscillator is free to pick any phase despite the interaction with the optical

modes. The phase forms a classical gauge field with $U(1)$ symmetry. The gauge transformation

$$\phi \mapsto \phi + \chi_2 - \chi_1, \quad (5)$$

$$a_j \mapsto a_j e^{i\chi_j}, \text{ for } j = 1, 2, \quad (6)$$

generates a new valid solution of the dynamical equations, for any real functions $\chi_j(t)$. The transformation also preserves optical and mechanical frequencies whenever it is time-independent, i.e., $\chi_j = \text{const}$. However, if χ_j are time-dependent, Eqs. (5) and (6) have to be supplemented by a shift in frequencies: $\Omega \mapsto \Omega + \dot{\chi}_1 - \dot{\chi}_2$ and $\nu_j \mapsto \nu_j - \dot{\chi}_j$. We will now show that any time-evolving phase ϕ can be viewed as generating a synthetic electric field

$$\mathcal{E} = \dot{\phi} \quad (7)$$

for photons. For example, if mode 1 is driven, we can re-gauge using $\chi_1 = 0$, $\chi_2 = -\phi$, which results in a description where the mechanical phase is static but $\nu_2 \mapsto \nu_2 + \mathcal{E}$. This describes an effective optical frequency shift, which can be interpreted as a synthetic electric field for photons in the same way that an energy difference between electronic levels indicates a voltage drop, i.e., a real electric field. In conventional electromagnetism, an electric field can be represented either as a time-dependent vector potential or a scalar potential gradient. Analogously, the synthetic electric field is described either by the time-evolution of the mechanical phase or by an effective frequency shift. As we will show, \mathcal{E} has important consequences for photon transport.

Dynamical phase diagram. — In the situation studied here, \mathcal{E} is not prescribed externally but it arises due to the dynamics of coupled optical and mechanical modes. The

optical modes induce the force F acting on the mechanical phase. The resulting phase evolution may generate a field \mathcal{E} which effectively modifies the optical frequency difference and, consequently, the population of the optical modes.

The results of the dynamical analysis are shown in Fig. 2. The results were obtained by linear stability analysis and numerical simulations of the equations of motion.

We consider the fully resonant situation where physical effects are most pronounced, as both optical driving and phonon-assisted photon tunneling are resonant ($\Delta_M = \Delta_1 = \Delta_2 = 0$). The system always converges to a steady state for any values of the parameters B , J , E , and κ . The steady-state value of \mathcal{E} depends on two dimensionless parameters: the rescaled limit-cycle amplitude BJ/κ and the rescaled laser amplitude EJ/κ^2 .

The dynamical analysis is made more intuitive by “integrating out” optical modes. This leaves us with an effective potential $V(\mathcal{E})$, whose minima determine steady-state values of \mathcal{E} (see Ref [57] for the full analytical expression):

$$\dot{\mathcal{E}} = -\frac{dV(\mathcal{E})}{d\mathcal{E}} = 0. \quad (8)$$

In the white region of the phase diagram, Fig. 2c, the potential $V(\mathcal{E})$ has a single minimum at $\mathcal{E} = 0$ (see the blue inset). For the lower-frequency mode, a_1 , being driven, this steady state becomes unstable in the colored region of the phase diagram, where the potential $V(\mathcal{E})$ has two minima at finite values of \mathcal{E} . The field \mathcal{E} can develop such a nonzero value for $B < E/\kappa$ (above the dashed orange line). In terms of physical parameters, this means that the occupation of the driven optical mode has to exceed the phonon number in the limit-cycle oscillation.

In contrast, if the higher-frequency mode, a_2 , is driven, $V(\mathcal{E})$ *always* has a single minimum at $\mathcal{E} = 0$ for any values of system parameters.

The states are not qualitatively changed for finite mechanical and laser detunings (see Ref. [57]).

We now study effects of the dynamically generated synthetic electric field on light transport. The transmission T is the ratio of the output power leaking from the non-driven mode, $\kappa|a_2|^2$ (if mode 1 is driven) or $\kappa|a_1|^2$ (if mode 2 is driven), and the driving power E^2/κ . We find that

$$T = \frac{\frac{B^2 J^2}{\kappa^2}}{\left(\frac{B^2 J^2}{\kappa^2} + \frac{1}{4}\right)^2 + \frac{1}{4\kappa^2} \mathcal{E}^2} \quad (9)$$

is suppressed when a finite field \mathcal{E} detunes the tunneling process from resonance. In Figs. 2d and 2e, \mathcal{E} and T , respectively, are depicted along the cut in Fig. 2c denoted by the dashed black line.

We have demonstrated for the two-site system that when light propagates to higher optical frequencies, the phonon-assisted photon tunneling is suppressed due to

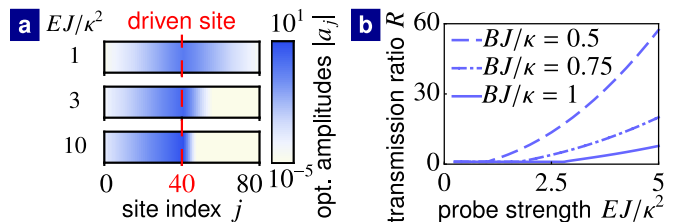


FIG. 3. Light transport in a 1D array with dynamical gauge fields – generation of a barrier for photon transport induced by synthetic electric fields. (a) The optical amplitudes $|a_j|$ as a function of position for different values of the laser amplitude E and $BJ/\kappa = 1$ (shown on a logarithmic scale). The dashed red line denotes the driven site. Transport to the right is strongly suppressed. (b) The ratio $R = |a_{d-1}/a_{d+1}|^2$ of the optical amplitudes adjacent to the driven site $j = d$. (Plotted for $n = 81$ sites, site $d = 40$ being driven.)

the synthetic electric field. In contrast, the field always vanishes when light propagates towards lower optical frequencies. In this way, dynamical gauge fields give rise to a new mechanism for unidirectional light transport. In the following, we demonstrate this effect in one-dimensional arrays.

Nonlinear unidirectional light transport in a one-dimensional array. — The physics of synthetic electric fields also affects photon transport in arrays (Fig. 1b). For more details see Ref. [57].

Fig. 3a shows the result for a 1D array: for a sufficiently large laser drive, the system switches into a state where finite \mathcal{E} develops to the right of the laser drive. This is the direction where photons need to gain energy when tunneling, and where we already saw in the two-site system that (i) a finite field can develop, and (ii) it suppresses photon transport. In the array, this results in a rapid exponential suppression of light intensity. In contrast, light easily propagates towards the left, where \mathcal{E} remains zero. In Fig. 3b, we plot the ratio $R = |a_{d-1}/a_{d+1}|^2$ of transmission to the sites adjacent to the driven site $j = d$ as a function of EJ/κ^2 . The suppression of light propagation to the right, i.e., $R > 1$, is achieved above the threshold of the laser amplitude. At m sites distance from the driven site, the ratio is exponentially increased to R^m .

Our numerical simulations indicate that unidirectional light propagation can also be observed in two-dimensional square arrays. In the future, one might study how these phenomena affect synchronization dynamics of coupled optomechanical self-oscillators [18, 58, 59].

Experimental parameters required for generating the synthetic electric field. — We now estimate that unidirectional light transport can be observed for experimentally realistic parameters. For the membrane-in-the-middle setup, feasible parameters are $\kappa \approx 300$ kHz, $J \approx 1$ Hz, a zero-point fluctuation amplitude of $x_{\text{ZPF}} \approx 10^{-15}$ m and a number of photons in the cavity $(E/\kappa)^2 \sim 10^{10}$ [52]. A typical phonon number in limit-cycle oscillations driven well above threshold is $B^2 \sim (\kappa/J)^2 \sim 10^{10}$ with a cor-

responding real oscillation amplitude $2x_{\text{ZPF}}B \sim 100$ pm [56]. Optical modes can be represented by hybridized transverse modes of a cavity with avoided crossing [52]. The splitting of their frequencies ≈ 200 kHz can match the mechanical frequency. For these experimental parameters, $EJ/\kappa^2 \sim 1$ and $BJ/\kappa \sim 1$ are promising for observing unidirectional light transport (see Fig. 2). The phonon number can be decreased below the photon number in the driven mode by driving mechanical self-oscillations closer to threshold [56], fulfilling the necessary condition for a finite synthetic electric field (Fig. 2).

Conclusions. — While synthetic gauge fields for photons have been investigated thoroughly in recent years, little has been known about the dynamical situation.

In this work, we have uncovered how a synthetic electric field can be spontaneously created in a readily realizable optomechanical setup. The resulting nonlinear photon-diode type of unidirectional transport can lead to a large isolation ratio, especially in arrays. In general, we demonstrate how the interplay of nonlinearity, dynamics, and artificial gauge fields can produce novel physical effects and possible new devices.

We thank A. Nunnenkamp and J. Harris for useful comments, and O. Hart for a careful reading of the manuscript. This work was supported by the European Union's Horizon 2020 research and innovation programme under grant agreement No 732894 (FET Proactive HOT).

-
- [1] M. Aspelmeyer, T. J. Kippenberg, and F. Marquardt, *Rev. Mod. Phys.* **86**, 1391 (2014).
- [2] J. Chan, T. P. M. Alegre, A. H. Safavi-Naeini, J. T. Hill, A. Krause, S. Gröblacher, M. Aspelmeyer, and O. Painter, *Nature* **478**, 89 (2011).
- [3] J. D. Teufel, T. Donner, D. Li, J. W. Harlow, M. S. Allman, K. Cicak, A. J. Sirois, J. D. Whittaker, K. W. Lehnert, and R. W. Simmonds, *Nature* **475**, 359 (2011).
- [4] D. J. Wilson, V. Sudhir, N. Piro, R. Schilling, A. Ghadimi, and T. J. Kippenberg, *Nature* **524**, 325 (2015).
- [5] R. W. Andrews, R. W. Peterson, T. P. Purdy, K. Cicak, R. W. Simmonds, C. A. Regal, and K. W. Lehnert, *Nat. Phys.* **10**, 321 (2014).
- [6] H. Xu, D. Mason, L. Jiang, and J. G. E. Harris, *Nature* **537**, 80 (2016).
- [7] S. Hong, R. Riedinger, I. Marinković, A. Wallucks, S. G. Hofer, R. A. Norte, M. Aspelmeyer, and S. Gröblacher, *Science* **358**, 203 (2017).
- [8] M. Hafezi and P. Rabl, *Opt. Express* **20**, 7672 (2012).
- [9] M. Schmidt, S. Kessler, V. Peano, O. Painter, and F. Marquardt, *Optica* **2**, 635 (2015).
- [10] A. Metelmann and A. A. Clerk, *Phys. Rev. X* **5**, 021025 (2015).
- [11] J. Kim, M. C. Kuzuk, K. Han, H. Wang, and G. Bahl, *Nat. Phys.* **11**, 275 (2015).
- [12] Z. Wang, L. Shi, Y. Liu, X. Xu, and X. Zhang, *Sci. Rep.* **5**, 8657 (2015).
- [13] F. Ruesink, M.-A. Miri, A. Alù, and E. Verhagen, *Nat. Commun.* **7**, 13662 (2016).
- [14] K. Fang, J. Luo, A. Metelmann, M. H. Matheny, F. Marquardt, A. A. Clerk, and O. Painter, *Nat. Phys.* **13**, 465 (2017).
- [15] N. R. Bernier, L. D. Tóth, A. Koottandavida, M. A. Ioannou, D. Malz, A. Nunnenkamp, A. K. Feofanov, and T. J. Kippenberg, *Nat. Commun.* **8**, 604 (2017).
- [16] S. Barzanjeh, M. Wulf, M. Peruzzo, M. Kalaei, P. B. Dieterle, O. Painter, and J. M. Fink, *Nat. Commun.* **8**, 953 (2017).
- [17] D. E. Chang, A. H. Safavi-Naeini, M. Hafezi, and O. Painter, *New J. Phys.* **13**, 023003 (2011).
- [18] G. Heinrich, M. Ludwig, J. Qian, B. Kubala, and F. Marquardt, *Phys. Rev. Lett.* **107**, 043603 (2011).
- [19] A. Xuereb, C. Genes, and A. Dantan, *Phys. Rev. Lett.* **109**, 223601 (2012).
- [20] M. Ludwig and F. Marquardt, *Phys. Rev. Lett.* **111**, 073603 (2013).
- [21] V. Peano, C. Brendel, M. Schmidt, and F. Marquardt, *Phys. Rev. X* **5**, 031011 (2015).
- [22] D. Jaksch and P. Zoller, *New J. Phys.* **5**, 56 (2003).
- [23] Y.-J. Lin, R. L. Compton, K. Jiménez-García, J. V. Porto, and I. B. Spielman, *Nature* **462**, 628 (2009).
- [24] M. Aidelsburger, M. Atala, S. Nascimbène, S. Trotzky, Y.-A. Chen, and I. Bloch, *Phys. Rev. Lett.* **107**, 255301 (2011).
- [25] M. Aidelsburger, M. Atala, M. Lohse, J. T. Barreiro, B. Paredes, and I. Bloch, *Phys. Rev. Lett.* **111**, 185301 (2013).
- [26] F. D. M. Haldane and S. Raghu, *Phys. Rev. Lett.* **100**, 013904 (2008).
- [27] Z. Wang, Y. Chong, J. D. Joannopoulos, and M. Soljačić, *Nature* **461**, 772 (2009).
- [28] M. Hafezi, E. A. Demler, M. D. Lukin, and J. M. Taylor, *Nat. Phys.* **7**, 907 (2011).
- [29] K. Fang, Z. Yu, and S. Fan, *Nat. Photonics* **6**, 782 (2012).
- [30] M. C. Rechtsman, J. M. Zeuner, A. Tünnermann, S. Nolte, M. Segev, and A. Szameit, *Nat. Photonics* **7**, 153 (2013).
- [31] M. Hafezi, S. Mittal, J. Fan, A. Migdall, and J. M. Taylor, *Nat. Photonics* **7**, 1001 (2013).
- [32] S. Mittal, J. Fan, S. Faez, A. Migdall, J. M. Taylor, and M. Hafezi, *Phys. Rev. Lett.* **113**, 087403 (2014).
- [33] L. M. Nash, D. Kleckner, A. Read, V. Vitelli, A. M. Turner, and W. T. M. Irvine, *Proc. Natl. Acad. Sci. U.S.A.* **112**, 14495 (2015).
- [34] R. Süssstrunk and S. D. Huber, *Science* **349**, 47 (2015).
- [35] P. Wang, L. Lu, and K. Bertoldi, *Phys. Rev. Lett.* **115**, 104302 (2015).
- [36] C. Brendel, V. Peano, O. J. Painter, and F. Marquardt, *Proc. Natl. Acad. Sci. U.S.A.* **114**, E3390 (2017).
- [37] C. Brendel, V. Peano, O. Painter, and F. Marquardt, *Phys. Rev. B* **97**, 020102 (2018).
- [38] A. Seif, W. DeGottardi, K. Esfarjani, and M. Hafezi, *Nat. Commun.* **9**, 1207 (2018).
- [39] N. Goldman, G. Juzeliūnas, P. Öhberg, and I. B. Spielman, *Rep. Prog. Phys.* **77**, 126401 (2014).
- [40] M. J. Hartmann, *J. Opt.* **18**, 104005 (2016).
- [41] S. Walter and F. Marquardt, *New J. Phys.* **18**, 113029

- (2016).
- [42] D. Banerjee, M. Dalmonte, M. Müller, E. Rico, P. Stebler, U.-J. Wiese, and P. Zoller, *Phys. Rev. Lett.* **109**, 175302 (2012).
 - [43] E. Zohar, J. I. Cirac, and B. Reznik, *Rep. Prog. Phys.* **79**, 014401 (2016).
 - [44] D. Marcos, P. Rabl, E. Rico, and P. Zoller, *Phys. Rev. Lett.* **111**, 110504 (2013).
 - [45] D. Marcos, P. Widmer, E. Rico, M. Hafezi, P. Rabl, U. J. Wiese, and P. Zoller, *Annals of Physics* **351**, 634 (2014).
 - [46] K. E. Ballantine, B. L. Lev, and J. Keeling, *Phys. Rev. Lett.* **118**, 045302 (2017).
 - [47] P. Hauke, D. Marcos, M. Dalmonte, and P. Zoller, *Phys. Rev. X* **3**, 041018 (2013).
 - [48] E. A. Martinez, C. A. Muschik, P. Schindler, D. Nigg, A. Erhard, M. Heyl, P. Hauke, M. Dalmonte, T. Monz, P. Zoller, and R. Blatt, *Nature* **534**, 516 (2016).
 - [49] L. Yuan and S. Fan, *Phys. Rev. Lett.* **114**, 243901 (2015).
 - [50] L. Yuan and S. Fan, *Optica* **3**, 1014 (2016).
 - [51] J. D. Thompson, B. M. Zwickl, A. M. Jayich, F. Marquardt, S. M. Girvin, and J. G. E. Harris, *Nature* **452**, 72 (2008).
 - [52] J. C. Sankey, C. Yang, B. M. Zwickl, A. M. Jayich, and J. G. E. Harris, *Nat. Phys.* **6**, 707 (2010).
 - [53] A. H. Safavi-Naeini and O. Painter, *New J. Phys.* **13**, 013017 (2011).
 - [54] T. K. Paraïso, M. Kalaei, L. Zang, H. Pfeifer, F. Marquardt, and O. Painter, *Phys. Rev. X* **5**, 041024 (2015).
 - [55] H. Wu, G. Heinrich, and F. Marquardt, *New J. Phys.* **15**, 123022 (2013).
 - [56] F. Marquardt, J. G. E. Harris, and S. M. Girvin, *Phys. Rev. Lett.* **96**, 103901 (2006).
 - [57] See supplementary material for the derivation of the effective potential for the sythetic electric field and the equations of motion for the one-dimensional array..
 - [58] R. Lauter, C. Brendel, S. J. M. Habraken, and F. Marquardt, *Phys. Rev. E* **92**, 012902 (2015).
 - [59] T. Weiss, S. Walter, and F. Marquardt, *Phys. Rev. A* **95**, 041802 (2017).

Dynamically generated Synthetic Electric Fields for Photons – Supplementary material

PHONON-ASSISTED PHOTON TUNNELING

In this section, we remark briefly on the derivation of the fundamental photon-phonon interaction term $\hat{b}\hat{a}_2^\dagger\hat{a}_1$ assumed in the Hamiltonian that describes our scenario. This term is actually obtained rather directly in optomechanical systems with two (or more) optical modes. Qualitatively, this term will arise whenever there are two optical modes that couple to the same mechanical resonator, and the term becomes important dynamically if the mechanical frequency matches the optical frequency difference. The earliest, well-known example is the membrane-in-the-middle setup of the Harris group [51, 52]. In the simplest case, if the membrane is placed exactly in the middle between the end mirrors of a cavity, the two optical modes \hat{a}_L and \hat{a}_R to the left and right of the membrane will be resonant. Therefore, they re-arrange into new symmetric and anti-symmetric optical eigenmodes, $\hat{a}_{1,2} = \frac{1}{\sqrt{2}}(\hat{a}_L \pm \hat{a}_R)$. As a consequence, the initial interaction transforms in the following way:

$$\left(\hat{a}_L^\dagger\hat{a}_L - \hat{a}_R^\dagger\hat{a}_R\right)(\hat{b} + \hat{b}^\dagger) = \left(\hat{a}_1^\dagger\hat{a}_2 + \hat{a}_2^\dagger\hat{a}_1\right)(\hat{b} + \hat{b}^\dagger). \quad (\text{S1})$$

Now, if mode '2' is the higher frequency mode, then (in rotating-wave approximation) only the terms $\hat{a}_2^\dagger\hat{a}_1\hat{b} + \text{h.c.}$ will be important for the dynamics. Although we assumed the perfectly symmetric situation for simplicity, the final result will still hold even if the initial optical modes were not perfectly resonant and therefore the new eigenmodes are not symmetric/anti-symmetric modes but carry more weight in one or the other half of the cavity. This only renormalizes the prefactor of the interaction term (according to the overlap of the new eigenmodes with the original modes).

Thus, in summary, whenever two optical modes and one mechanical resonator are in mutual interaction, and when the mechanical frequency matches the optical frequency difference (at least approximately), the interaction term $\hat{a}_2^\dagger\hat{a}_1\hat{b} + \text{h.c.}$ assumed in our work is the generic outcome.

STEADY STATES OF THE TWO-SITE SYSTEM

In this section, we analyze the steady states of the two-site system with single mode being driven. They are stationary solutions of the equations of motion (Eq. (2), Eq. (3), and Eq. (4) in the main text) constant in time. We first apply a time-dependent gauge transformation to express the time-evolution of the mechanical phase in a form of an effective optical frequency shift. Then we find a stationary condition for the synthetic electric field \mathcal{E} . Finally, we use an effective potential for the synthetic electric field to study stability of its stationary solutions.

As mentioned in the main text, we assume that only one mode is driven. We label the driven mode by the index $k = 1, 2$. Driving strengths can then be expressed as $E_j = E\delta_{j,k}$ for $j = 1, 2$, where $\delta_{j,k}$ is the Kronecker delta. The detuning of the non-driven mode can be set to zero, since there is no driving frequency. Therefore, the optical detunings can be expressed as $\Delta_j = \Delta_O\delta_{j,k}$. We make use of the time-dependent gauge transformation

$$\phi = \tilde{\phi} + \chi, \quad (\text{S2})$$

$$a_1 = \tilde{a}_1 e^{-i\chi\delta_{2,k}}, \quad (\text{S3})$$

$$a_2 = \tilde{a}_2 e^{i\chi\delta_{1,k}}, \quad (\text{S4})$$

which moves the dynamics of the mechanical phase to the time-dependent gauge parameter χ . By appropriately choosing χ , we can always achieve $\tilde{\phi} = 0$. The time-dependent gauge transformation leaves the absolute values of the optical amplitudes unchanged. As a result, a particular value of the gauge parameter is irrelevant. Only its first derivative $\dot{\chi} = \dot{\phi}$ influences the optical occupations. The time evolution of the mechanical phase results in an effective shift $(\delta_{2,k} - \delta_{1,k})\dot{\chi}$ of the non-driven optical mode's frequency. Note that the driven mode, a_k , is forced to oscillate with the frequency of the laser drive, and thus it does not experience any frequency shift.

The role of the optical frequency shift $\dot{\chi}$ can be understood in analogy to electromagnetism. The mechanical phase corresponds to an effective vector potential. According to conventional electromagnetism, the time evolution of the vector potential generates an electric field. This electric field can be also represented by a scalar potential gradient. In this analogy, the time evolution of the mechanical phase generates a synthetic electric field $\mathcal{E} = \dot{\chi}$ for photons, which represent an effective optical frequency shift.

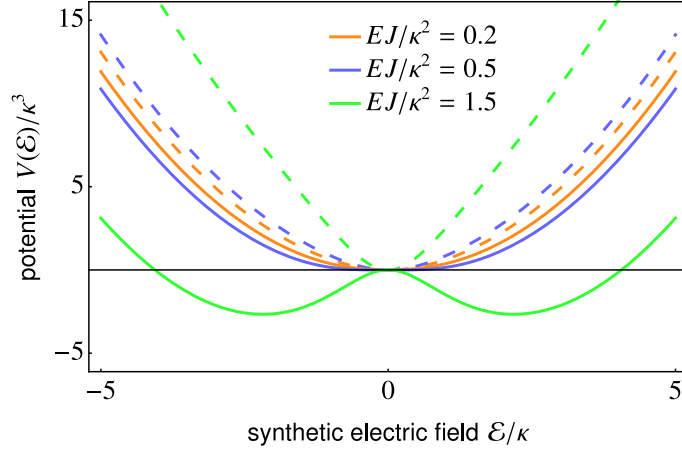


FIG. S1. The potential for the synthetic electric field. It has a single minimum at $\mathcal{E} = 0$ for $k = 2$ (dashed lines) when the higher optical frequency is driven. For $k = 1$, when the lower optical frequency is driven, the stationary value $\mathcal{E} = 0$ becomes unstable with increasing EJ/κ^2 as two minima with a finite frequency shift emerge (solid lines). (The potential is plotted for $BJ/\kappa = 0.5$.)

To provide the fixed point analysis for the both cases $k = 1, 2$ at once, we use general indexes $(k, l) \in \{(1, 2), (2, 1)\}$ to label the optical modes. According to the gauge transformation (S2), (S3), and (S4), the equations of motion transform to

$$\dot{\phi} = \mathcal{E} - \Delta_M + \frac{J}{B} \text{Re} [\tilde{a}_k^* \tilde{a}_l] = 0, \quad (\text{S5})$$

$$\dot{\tilde{a}}_k = i\Delta_O \tilde{a}_k - iE - iJB\tilde{a}_l - \frac{\kappa}{2} \tilde{a}_k, \quad (\text{S6})$$

$$\dot{\tilde{a}}_l = i(\delta_{2,k} - \delta_{1,k}) \mathcal{E} \tilde{a}_l - iJB\tilde{a}_k - \frac{\kappa}{2} \tilde{a}_l, \quad (\text{S7})$$

where we substituted $\mathcal{E} = \dot{\chi}$. Taking the time derivative of Eq. (S5), we obtain the equation of motion for the synthetic electric field

$$\dot{\mathcal{E}} = -\kappa(\mathcal{E} - \Delta_M) + \frac{EJ}{B} \text{Im} [\tilde{a}_l] + \frac{J}{B} ((\delta_{2,k} - \delta_{1,k}) \mathcal{E} - \Delta_O) \text{Im} [\tilde{a}_k^* \tilde{a}_l]. \quad (\text{S8})$$

To find stationary solutions of the equations of motion (S6), (S7), and (S8), we first use that the equations (S6) and (S7) are linear in terms of optical amplitudes. For a given value of the synthetic electric field \mathcal{E} , the stationary optical amplitudes read

$$\tilde{a}_k = E \frac{(\delta_{2,k} - \delta_{1,k}) \mathcal{E} + i\frac{\kappa}{2}}{-J^2 B^2 + (\delta_{2,k} - \delta_{1,k}) \mathcal{E} \Delta_O - (\frac{\kappa}{2})^2 + i\frac{\kappa}{2} [(\delta_{2,k} - \delta_{1,k}) \mathcal{E} + \Delta_O]}, \quad (\text{S9})$$

$$\tilde{a}_l = \frac{JB}{(\delta_{2,k} - \delta_{1,k}) \mathcal{E} + i\frac{\kappa}{2}} \tilde{a}_k. \quad (\text{S10})$$

In following, we set $\Delta_O = \Delta_M = 0$ to present the important features of the steady states. These features are not changed by finite detunings. We discuss the effects of finite detunings at the end of this section. By substituting the stationary values of the optical amplitudes (S9), (S10) into Eq. (S8), we obtain the stationary condition for the synthetic electric field

$$0 = \dot{\mathcal{E}} = -\kappa \mathcal{E} \frac{(\frac{\mathcal{E}}{\kappa})^2 + 4 \left[\left(\frac{JB}{\kappa} \right)^2 + \frac{1}{4} \right]^2 + 4(\delta_{2,k} - \delta_{1,k}) \left(\frac{EJ}{\kappa^2} \right)^2}{(\frac{\mathcal{E}}{\kappa})^2 + 4 \left[\left(\frac{JB}{\kappa} \right)^2 + \frac{1}{4} \right]^2}. \quad (\text{S11})$$

For $k = 2$, when the mode with the higher optical frequency, a_2 , is driven, only the single stationary solution, $\mathcal{E} = 0$, exists. For $k = 1$, when the mode with the lower optical frequency, a_1 , is driven, stationary solutions with a finite

synthetic electric field

$$\mathcal{E}_{\pm} = \pm 2\kappa \sqrt{\left(\frac{EJ}{\kappa^2}\right)^2 - \left[\left(\frac{JB}{\kappa}\right)^2 + \frac{1}{4}\right]^2} \quad (\text{S12})$$

emerge, in addition to $\mathcal{E} = 0$, for $4EJ/\kappa^2 > 4(BJ/\kappa)^2 + 1$.

To gain intuition about the stability of these stationary solutions, we find the potential

$$V(\mathcal{E}) = \frac{\kappa^3}{2} \left(\left(\frac{\mathcal{E}}{\kappa}\right)^2 + 4(\delta_{2,k} - \delta_{1,k}) \left(\frac{JE}{\kappa^2}\right)^2 \ln \left(\left(\frac{\mathcal{E}}{\kappa}\right)^2 + 4 \left[\left(\frac{JB}{\kappa}\right)^2 + \frac{1}{4} \right]^2 \right) \right), \quad (\text{S13})$$

such that $-dV(\mathcal{E})/d\mathcal{E}$ is equal to the right hand side of Eq. (S11). The potential shows that the stationary solution $\mathcal{E} = 0$ is always a stable steady state for $k = 2$ when the optical mode with the higher optical frequency is driven (see Fig. S1). The stability of the steady state does not depend on the system parameters. For $k = 1$, when the mode with the lower optical frequency is driven, the stability of the steady state depends on the two dimensionless parameters EJ/κ^2 and BJ/κ . The potential in Fig. S1 shows that the steady state $\mathcal{E} = 0$ is the only stationary solution and it is stable in the white region of the phase diagram depicted in Fig. 2 of the main text. It becomes unstable as the two steady states with a finite synthetic electric field emerge in the colored region of the phase diagram in Fig. 2 of the main text. Note that the potential does not provide conclusive information about the stability of the steady states because it does not take into account the dynamics of the optical modes. Therefore, the linear stability analysis was used to confirm that the stability of the steady states is determined correctly by the potential $V(\mathcal{E})$.

A finite mechanical detuning, $\Delta_M \neq 0$, detunes the phonon-assisted photon tunneling process from resonance. In this way, the mechanical detuning represents a static synthetic electric field for photons in contrast to the dynamically generated synthetic electric field \mathcal{E} . If the higher optical frequency is driven, the dynamically generated synthetic electric field \mathcal{E} acts against this static synthetic electric field and increases transmission to the lower optical frequency with the increasing laser amplitude. On the other hand, for the lower optical frequency being driven, the dynamically generated synthetic electric field detunes the tunneling process further from resonance with the increasing laser amplitude. As a result, it decreases light propagation to the non-driven optical mode. Above some threshold of the laser amplitude, the synthetic electric field bifurcates as the effective potential have two local minima. This again happens only for the lower frequency being driven.

A finite laser detuning, $\Delta_O \neq 0$, suppresses the coherent driving, which results in a smaller optical amplitude of the driven mode. For the higher optical frequency being driven, the synthetic electric field always vanishes even for a finite optical detuning. It vanishes also when the lower optical frequency is driven for small laser amplitudes. Similarly as in the resonant case, the synthetic electric field bifurcates to finite values over the threshold of the laser amplitude for the lower frequency being driven. The threshold and the values of the bifurcated synthetic electric field are modified by the finite optical detuning since it changes the population and the phase of the driven optical mode. However, the qualitative features of the synthetic electric field remain the same. The synthetic electric field is generated only above threshold and only for the lower optical frequency being driven.

PHASE LOCKING

In this section, we provide a brief summary of phase locking, which can be reached in the two site system by simultaneously driving both optical modes. Note that the analysis presented in the main text is for a single mode driven only. We present here quantitative features of phase locking, which has been previously well studied in a similar optomechanical system [18].

The starting point of the analysis are the equations of motion (2), (3) and (4) in the main text. The stationary values for the optical amplitudes are

$$a_1 = -\frac{JBE_2e^{-i\phi} + i\frac{\kappa}{2}E_1}{J^2B^2 + \left(\frac{\kappa}{2}\right)^2}, \quad (\text{S14})$$

$$a_2 = -\frac{JBE_1e^{i\phi} + i\frac{\kappa}{2}E_2}{J^2B^2 + \left(\frac{\kappa}{2}\right)^2}. \quad (\text{S15})$$

Note that if both optical modes are driven, the phases φ_1 and φ_2 of the laser amplitudes E_1 and E_2 , respectively, determine the phases θ_1 and θ_2 of the intracavity modes. This is different to the case when only a single optical mode is driven, where the phase of the driving amplitude is irrelevant.

The stationary value of the mechanical phase ϕ obeys the Adler equation

$$\Delta_M - |a_1||a_2| \cos(\phi - \theta) = 0. \quad (\text{S16})$$

where $\theta = \theta_2 - \theta_1$. However, the absolute values of the optical amplitudes $|a_1|$ and $|a_2|$ depend on the phase difference $\phi - \theta$. The Adler equation still determines uniquely the stationary value of $\cos(\phi - \theta)$ but the full analytical expression of this equation is complicated. Thus it is simpler to switch to the phase difference $\varphi = \varphi_2 - \varphi_1$ of the laser phases φ_1 and φ_2 . The Adler equation then has the form

$$\Delta_M - \frac{J}{B} \frac{|E_1||E_2|}{J^2 B^2 + \left(\frac{\kappa}{2}\right)^2} \cos(\phi - \varphi) = 0. \quad (\text{S17})$$

We can easily read off that the stationary solution of ϕ exists for

$$|\Delta_M| \leq \frac{J}{B} \frac{|E_1||E_2|}{J^2 B^2 + \left(\frac{\kappa}{2}\right)^2}. \quad (\text{S18})$$

The mechanical phase ϕ is locked under this condition to the difference φ of the laser drives' phases. Since there is one-to-one correspondence between the laser drives' phases and the intracavity modes' phases, the mechanical phase ϕ can be equivalently though to be locked to the phase difference θ of the intracavity modes.

ONE-DIMENSIONAL ARRAYS

Here we provide details about one-dimensional arrays analyzed in the main text. We consider an array, depicted in Fig. 1b of the main text, represented by a stack of membranes inside a cavity. The sites of the array support optical modes a_j whose frequencies ν_j increase with site index $j = 1, \dots, n$. We assume that the phonon-assisted photon tunneling processes are resonant: $\Omega_j = \nu_{j+1} - \nu_j$, where Ω_j is the frequency of the mechanical oscillator assisting tunneling between modes \hat{a}_j and \hat{a}_{j+1} . Specifically, we will consider a situation where some optical mode $j = d$ is driven resonantly from the side, to study light propagation towards the left ($j < d$), and towards the right ($j > d$). Alternatively to membrane stacks, suitably designed coupled cavity arrays in optomechanical crystals could implement such a setup.

The mechanical oscillators are again assumed to perform limit cycle oscillations $\langle \hat{b}_j \rangle = B e^{i\phi_j}$ with free phases and with a fixed amplitude B equal for all mechanical oscillators. By straightforward extension of Eqs. (2), (3), and (4) (in the main text), we obtain the coupled equations of motion for the optical amplitudes and the mechanical phases

$$\dot{\phi}_j = -\frac{J}{B} \text{Re} [a_j^* a_{j+1} e^{-i\phi_j}], \quad (\text{S19})$$

$$\dot{a}_j = -iE_j \delta_{j,d} - iJB e^{-i\phi_j} a_{j+1} - iJB e^{i\phi_{j-1}} a_{j-1} - \frac{\kappa}{2} a_j, \quad (\text{S20})$$

where $\delta_{j,d}$ is the Kronecker delta. The optical modes are expressed in the frames rotating with their frequencies ν_j and the mechanical modes are in the frames rotating with the difference of optical frequencies on the neighboring sites: $\nu_{j+1} - \nu_j$.

We study the dynamics of one-dimensional arrays by numerically solving the classical equations of motion (S19) and (S20). The system converges to a steady state for any values of the parameters EJ/κ^2 and BJ/κ . Properties of the steady states are discussed in the main text.